Available online at www.sciencedirect.com
SCIENCE DIRECT®
Journal of Crystal Growth 264 (2004) 379–384
JOURNAL OF CRYSTAL GROWTH
www.elsevier.com/locate/jcrysgro

Long-time scale morphological dynamics near the onset of instability during directional solidification of an alloy

C.W. Lan*, C.J. Shih, W.T. Hsu

Department of Chemical Engineering, National Taiwan University, No. 1, Sec. 4, Rossevelt Road, Taipei 10617, Taiwan

Received 10 December 2003; accepted 11 December 2003
Communicated by G.B. Stringfellow

Abstract

The long-time scale nonlinear morphological dynamics of the interface during the thin-film directional solidification of an SCN/acetone alloy have been simulated by an efficient phase field simulation. In addition to the agreement with classic theories, the mode transition ($\lambda_c \leftrightarrow \lambda_c/2$) through periodic–chaotic–periodic solute pinch-off after a step change of the solidification speed is illustrated; λ_c is the critical wavelength. The tip-splitting, coarsening, and overshooting during mode transition are consistent with experimental observations. However, the transition time is up to $5D_L/kV^2$ making a real experiment at lower solidification speed very difficult to perform, where D_L is the acetone diffusivity, k the segregation coefficient, and V the solidification speed. The subcriticality of the primary bifurcation is further confirmed by simulation.

PACS: 68.70.+w; 81.30.Fb

Keywords: A1. Directional solidification; A1. Morphological instability; A1. Phase field simulation

The onset of instability from a planner to a cellular structure has very rich nonlinear dynamics and has been paid much attention since the classical Mullins–Sekerka (MS) theory was proposed [1]. Warren and Langer [2] further extended the analysis to predict the onset wavelength, with some success, from a planar to a cellular morphology subjected to a step change of the solidification velocity. However, the prediction of the detailed nonlinear morphological development remains a challenging problem in microstructure pattern formation. It is indeed a difficult problem not only for simulation, but also for experiments. The front-tracking method with bifurcation analyses has shown some progress [3], but it has failed to simulate the problem having interface merging or separation, such as pinching off. Phase field simulation has emerged as a powerful tool for this category of problems. However, a quantitative simulation of alloy solidification is also difficult because of the problems on the length and time scales for computation. An extremely small interface thickness is required to reduce solute trapping, while a large domain is required to accommodate the solute and thermal boundary layers. On the other hand, near the onset of the morphological instability, the solidification rate is

*Corresponding author. Tel./fax: +886-2-2218-89088.
E-mail address: cwlan@ntu.edu.tw (C.W. Lan).

0022-0248/$ - see front matter © 2003 Elsevier B.V. All rights reserved.
doi:10.1016/j.jcrysgro.2003.12.032

small, and the time scale for morphological dynamics becomes extremely large. Both seem to greatly discourage the use of phase field simulation for further comparison with the classic theories and experiments. Furthermore, the long-time scale experiments are difficult to perform because of the requirements of large system scale and high sample purity. To reduce the time and length scales for the experiments, a much lower solute concentration is required for observing the detailed mode transitions near the onset point. Besides, the speed range for mode transition decreases with the increasing of solute concentration [1]. Therefore, even for the most common transparent succinonitrile (SCN)/acetone system, the experiments for the long-time scale morphological dynamics near the onset of the instability has not yet been reported, and so as the phase field simulation of the problem.

In the MS theory, the equilibrium is assumed at the interface. Therefore, the segregation coefficient k is constant. However, if the interface is diffusive, solute drag appears in the interface, and the solute trapping depends on the velocity V and the interface thickness δ as pointed out by Aziz [4] and Ahmad et al. [5]. The effective segregation coefficient k_{eff} was derived as

$$k_{\mathrm{eff}} = \frac{k + V/V_{\mathrm{D}}}{1 + V/V_{\mathrm{D}}}, \tag{1}$$

where V_{D} is the interface diffusion speed and can be represented as $V_{\mathrm{D}} = 0.207\, D_{\mathrm{L}} \ln(1/k)/\delta(1-k)$ [4], where D_{L} is the solute diffusivity in the melt. To minimize the solute trapping, while to balance computing load, the interface thickness cannot be too small, and this requires a lower solidification. Unfortunately, at a lower speed, the time scale for the interface dynamics, being in the order of D_{L}/V^2, becomes very large. In a recent analysis by Warren and Langer [2], the time for the interface to fully develop is much longer than that for the solute boundary layer and is in the order of several D_{L}/kV^2. In other words, for most solutes, k is in the order of 0.1 or smaller, so that the time scale for the morphological dynamics is extremely long. Therefore, an efficient numerical solution requite adaptive mesh refinement (AMR) that allocates enough mesh for the interface and solute boundary layer, while uses much less grids for the rest of the domain. Taking SCN with 0.2 mol% acetone ($k = 0.1$) as an example, several hours are needed for the morphological development. On the other hand, as shown in the stability diagram obtained from Mullens and Sekerka [1], as shown in Fig. 1, the speed range for mode transition is very small at this composition, so that for most available experiments the detailed nonlinear dynamics near the onset are very difficult to capture. The mode transition from the onset wavelength λ_{c} to $\lambda_{\mathrm{c}}/2$ is within 1% of the onset speed V_{c}. However, if the concentration is reduced to 0.01 wt%, the transition spans over 10% of V_{c} or 80% for the $\lambda_{\mathrm{c}}/4$ mode. This is also true for simulation. Therefore, in this paper, we have purposely reduced the solute concentration to 0.01 wt%, and performed phase field simulation to illustrate the lone-time scale nonlinear dynamics of the morphological evolution. As will be illustrated shortly, quantitative comparison with the theories is possible. Meanwhile, a full transition from λ_{c} to $\lambda_{\mathrm{c}}/2$ and then back to λ_{c} by changing the speed up and down can be found. Some interesting phenomena are observed and are consistent with experiments.

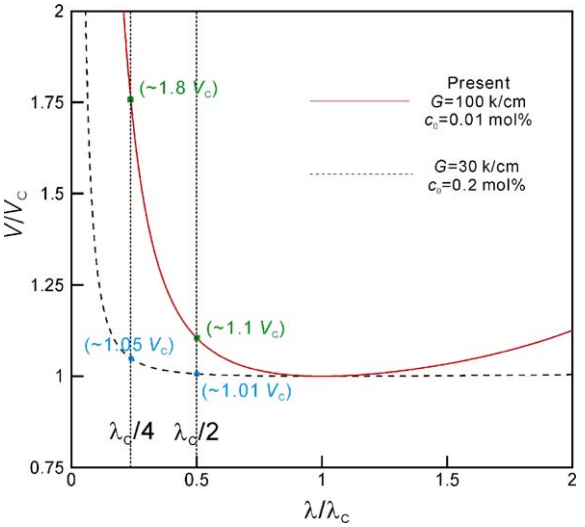

Fig. 1. A portion of the normalized MS loop showing the onset solidification speed as a function of cellular wavelength for two different conditions.

The phase field simulation is based on the WBM model [6]. The frozen temperature approximation (FTA) is adopted having a thermal gradient G.

FTA is not realistic here based on the heat flow consideration. However, to focus on solute transport and the comparison with the previous studies, this assumption is still adopted here. In order to present the governing equations in dimensionless form, the variables are rescaled. The concentration (atomic fraction) c is rescaled by c_0 to c^*, where c_0 is the far field concentration. The coordinates x and y are rescaled by the interface thickness δ to x^* and y^*, respectively, and time t by δ^2/D_L to t^*. The phase filed variable ϕ is set to be 1 in liquid and 0 in solid, while 0.5 at the interface. The steady solidification speed V is rescaled by D_L/δ to V^*. Then, the governing equations used can be represented in dimensionless form [7]:

$$\frac{\partial\phi}{\partial t^*} - V^*\frac{\partial\phi}{\partial y^*} = M_\phi^*\varepsilon^{*2}\left[\nabla\cdot\left(\eta^2\nabla\phi\right) - \frac{\partial}{\partial x}\left(\eta\eta_\beta\frac{\partial\phi}{\partial y}\right) + \frac{\partial}{\partial y}\left(\eta\eta_\beta\frac{\partial\phi}{\partial x}\right)\right] - M_\phi^* S^*, \quad (2)$$

$$\frac{\partial c*}{\partial t*} - V^*\frac{\partial c^*}{\partial y^*} = \nabla\cdot\left\{D^*\left[\nabla c + c^*\left(1-c_0c^*\right)\times\left(S_B^* - S_A^*\right)\nabla\phi\right]\right\}. \quad (3)$$

The physical properties of pure SCN and acetone are applied to form an ideal alloy solution assumed in the WBM model. The only exception is the latent heat of acetone ($9.651\times10^7\,\mathrm{J/m^3}$). It is modified to fit the measured segregation coefficient $k(0.1)$ and the liquidus slope m ($-222\,\mathrm{k/(mol\ fraction)}$). M_ϕ^*, ε^*, D^*, and S^* are the dimensionless mobility, parameter related to interfacial energy, diffusivity, and entropy of the alloy accounting the mixing rule for the melt and the solid. Also, S_A^* and S_B^* are the normalized entropy of A (solvent) and B (solute), respectively. The interface thickness δ is chosen as $0.2\,\mu\mathrm{m}$ to minimize solute trapping and balance the computational accuracy and load. The detailed description of the phase-field parameters can be found elsewhere [6]. The anisotropic function η in Eq. (2) is defined for the four-fold symmetry as

$$\eta = 1 + \gamma\cos 4\beta, \quad (4)$$

where γ is the intensity of the anisotropy (0.04 is used) and $\beta = \tan^{-1}[(\partial\phi/\partial y)/(\partial\phi/\partial x)]$ is the growth orientation of the cell.

To solve these equations, an adaptive finite volume method has been used. The detailed implementation of the scheme can be found elsewhere [8]. On the both sides of the domain, the symmetry (no flux) condition is used. On the top boundary, the concentration ($c^*=1$) is given, while at the lower boundary the concentration is set by the exit condition with its own concentration, i.e., $\partial c^*/\partial y^* = 0$.

Simulation is performed for SCN with 0.01 mol% acetone at a thermal gradient of 100 K/cm. Before the simulation is conducted, as shown in Fig. 1, the mode transition near the onset ($\lambda_c \leftrightarrow \lambda_c$ /4) occurs within a reasonable speed range, i.e., about 1–$2V_c$. At this speed range, the solutal trapping is small, and the maximum effect segregation coefficient is only about 0.12, which is very close to the equilibrium one ($k=0.1$). The decay length of the solute profile and the interface position after a step change of solidification speed at $50\,\mu\mathrm{m/s}$, which is less than V_c ($72.6\,\mu\mathrm{m/s}$), are calculated first. The results are in good agreement with the analytical solution derived by Warren and Langer [2]. More importantly, the solution field takes about D_L/kV^2 (~5 s) to reach a steady state. However, $5D_L/kV^2$ (~25 s) is required for the steady interface position. In other words, it is believed that it will take about the same order of time for the interface to develop. Increasing the velocity to $90\,\mu\mathrm{m/s}$, the interface remains planar even up to $10\,D_L/kV^2$ (15.68 s). However, changing the speed from 90 to $100\,\mu\mathrm{m}$, the interface becomes unstable after $5D_L/kV^2$ (6.35 s). A fully development of the morphology requires another $5D/kV^2$ and the wavelength is about $33.3\,\mu\mathrm{m}$, which is a λ_c/2 mode ($\lambda_c = 68.4\,\mu$); is taken from the MS theory. Similar simulations are performed by increasing the speed stepwise to $200\,\mu\mathrm{m/s}$, and then backward to $75\,\mu\mathrm{m/s}$. The average amplitude is also measured as shown in Fig. 2 showing the effects of solidification speed on the cell amplitude; some fully developed morphologies are also illustrated inside the figure. As shown, the λ_c mode can be obtained by reducing the speed, even though it is missed in the increasing speed. Interestingly, as shown there is a sudden increase on the cell depth when the speed is changed from 85 (a $\lambda_c/2$ mode) to $80\,\mu\mathrm{m/s}$ (a λ_c mode). By further reducing the

speed to 80 μm/s, the λ_c mode remains, but the amplitude decreases. The planar interface is obtained again when the speed is reduced to 75 μm/s. Interestingly, the time needs to smooth out the interface being about D/kV^2 is much shorter than that to develop. This figure clearly indicates the $\lambda_c \leftrightarrow \lambda_c/2$ mode transition is subcritical, which is as predicted by the theory [9] and observed in experiments [10]. This bifurcation diagram (Fig. 2) is quite similar to the one predicted by Lee et al. [11] using a finite element method for steady-state calculations [11]. However, there are some important features, which will be illustrated shortly, were not seen in the previous simulation or experiments. Fig. 3 shows the results on the MS loop. As shown, they are in pretty good agreement; a local view of the MS-loop in a normal scale is shown on the corner. At higher solidification speed (> 180 μm/s), a shorter-wavelength mode (near $\lambda_c/3$) is also found.

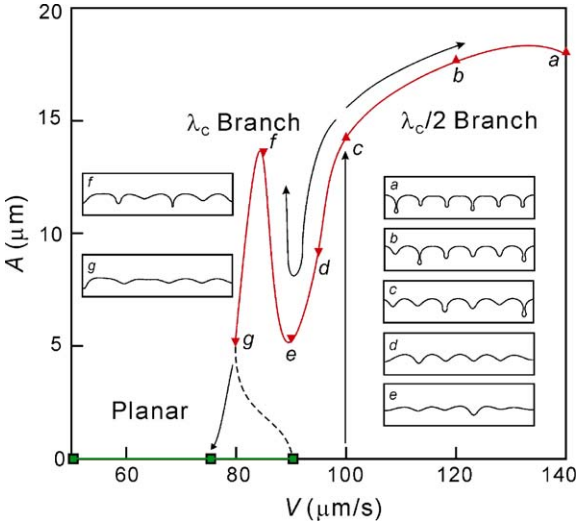

Fig. 2. Bifurcation diagram for the maximum cell amplitude (A) as a function of the solidification speed. The symbols upper and lower triangles represent the morphologies obtained by increasing and decreasing solidification speed, respectively, while the square symbols indicate the planar interface.

The interface dynamics during the previous mode transition are particularly interesting. For the onset of the instability (from 75 to 90 μm/s), it takes more than $10\,D_L/kV^2$ to a fully developed morphology. However, this morphology is having a periodic pinch-off structure, as shown in Fig. 4a. The solute is trapped in the deep groove and then pinched off forming a packet left behind the

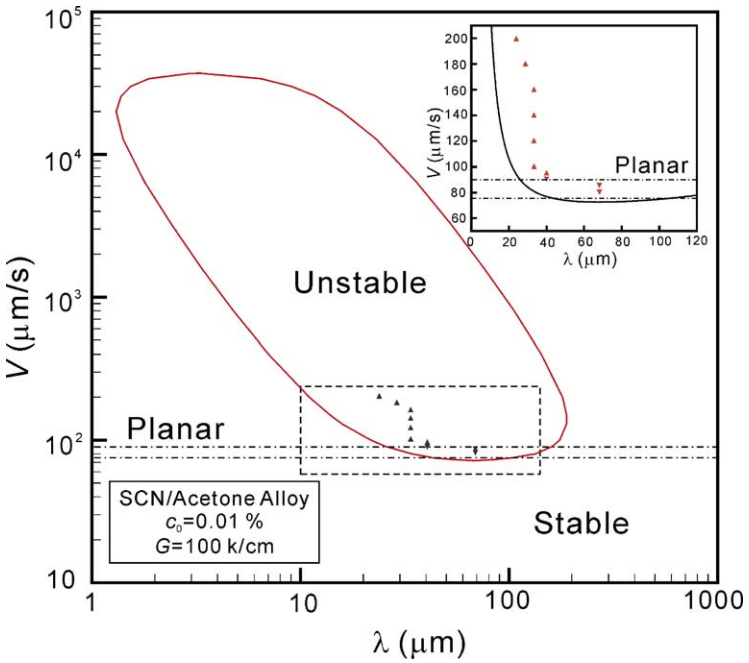

Fig. 3. Comparison of the simulated results with the MS loop.

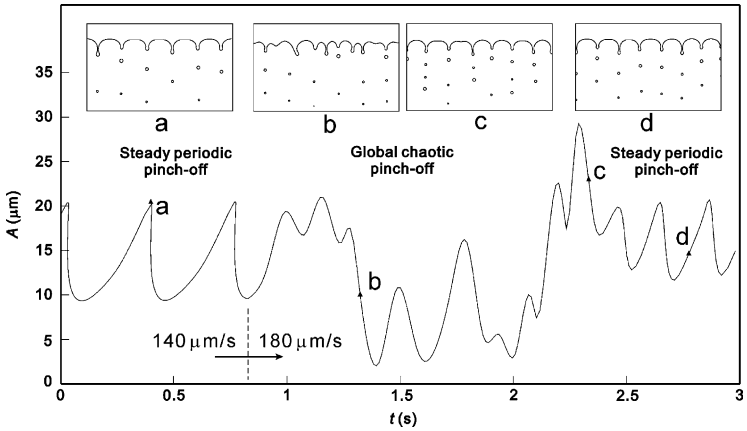

Fig. 4. Time evolution of cell amplitude after a step change of the solidification speed from 140 to 180 μm/s.

interface. These packets do not detached at the same time. However, the distance (pinch-off period) between the packets is the same for each groove. Increasing the speed to 180 μm/s, the pinch-off become chaotic, as shown in Figs. 4b and c. One can notice that the distance between the pinch-off packets from each groove is different from one another. After a new mode is developed, the periodic pinch-off structure appears again, as shown in Fig. 4d. If we plot the time evolution of a groove depth, as shown in Fig. 4, the nature of the interface dynamics can be easily understood. When the speed is increases, there is a temporary chaotic period before the new periodic pinch-off state. A similar transition appears at a high speed before turning to a global chaotic pinch-off situation. Moreover, as shown in Fig. 4, the transition through the global chaotic period takes more than 2 s, i.e., up to $5\,D_L/kV^2$, and this will take a real experiment having a much higher acetone concentration and lower solidification speed. For $c_0 \sim 0.3$ mol% and $V \sim 0.5$ μm/s, it will take about 50 h for the mode transition. Such kind of long-time scale experiments have not yet been performed. In addition to the long solidification setup, the decomposition of SCN at the hot zone is a problem as well [12].

During the transition, the interface shows clear tip coarsening, groove overshooting and pinching off, and tip splitting, as shown in Fig. 5. Some photographs from the experiments obtained from a higher acetone concentration and a lower solidification speed ($c_0 = 0.32$ mol%, $V = 0.589$ μm/s, $G = 30$ K/cm) are also shown. As shown, when two grooves, where solute accumulates, merge together (coarsening), the local solute concentration increases and forms a deeper groove (amplitude overshooting) with a pinch-off. After

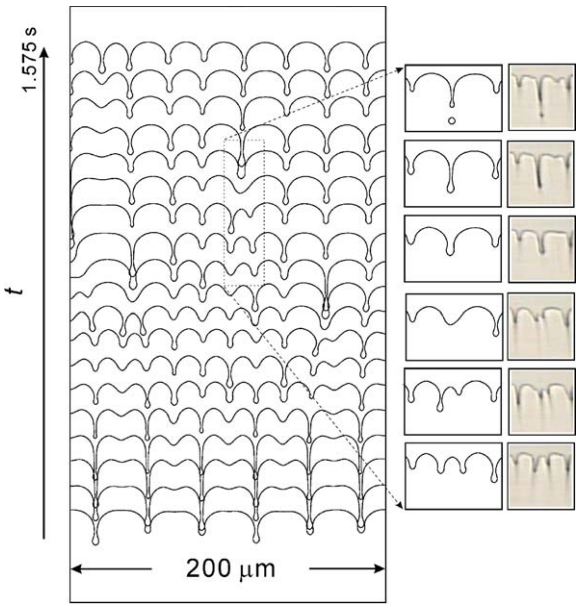

Fig. 5. Morphological transition after a step change of the solidification speed from 140 to 200 μm/s. The morphology at every 0.07825 s ($2.5\,D_L/V^2$) is shown. On the right the experimental photographs are also shown ($c_0 = 0.32$ mol%, $V = 0.589$ μm/s, and $G = 30$ K/cm; time interval = 50 min; total time = 250 min $\sim 4.2\,D_L/V^2$).

the pinch-off, the groove depth decreases quickly. On the other hand, as the merged interface is having a too long wavelength, splitting may occur. The time for the transition is about 0.4 s in the simulation, but about 250 min in the experiments. However, they are still quite consistent to each other based on the dimensionless time being about D_L/kV^2. Such a transition continues for several D_L/kV^2 until a new mode is fully developed. Nevertheless, the new mode is still time-dependent in nature. Again, this is a great challenge for a real experiment with a low solidification or high solute concentration.

In summary, the long-time scale nonlinear morphological dynamics near the onset of instability for a thin-film solidification of an SCN/acetone alloy have been simulated by phase field simulation. The results are in good agreement with the reported theories. The transition phenomena, such as tip splitting, cell coarsening, amplitude overshooting, and solute pinching-off, are consistent with the long-time scale experimental observations. The dimensionless time scale for the morphological evolution is also consistent with the measured one based on a higher acetone concentration and a lower solidification speed. However, the time to complete a morphological transition by increasing the solidification speed is up to $5D_L/kV^2$, which could take days in a real experiment.

The authors are grateful for the financial support from the National Science Council of the Republic of China.

References

[1] W.W. Mullins, R.F. Sekerka, J. Appl. Phys. 35 (1964) 444.
[2] J.A. Warren, J.S. Langer, Phys. Rev. E 47 (1993) 4072.
[3] K. Tsiveriotis, R.A. Brown, Phys. Rev. B 48 (1993) 13495.
[4] M.J. Aziz, T. Kaplan, Acta. Metall. 36 (1988) 2335.
[5] N.A. Ahmad, A.A. Wheeler, W.J. Boettinger, G.B. McFadden, Phys. Rev. E 58 (1998) 3436.
[6] A.A. Wheeler, W.J. Boettinger, G.B. MacFadden, Phys. Rev. A 45 (1992) 7424;
A.A. Wheeler, W.J. Boettinger, G.B. MacFadden, Phys. Rev. E 47 (1993) 1893.
[7] J.A. Warren, W.J. Boettinger, Acta Metall. Mater. A 43 (1995) 689.
[8] C.W. Lan, C.C. Liu, C.M. Hsu, J. Comp. Phys. 178 (2002) 464.
[9] D.J. Wollkind, L.A. Segel, Philos. Trans. Roy. Soc. London 268 (1970) 351.
[10] M.A. Eshelman, R. Trivedi, Acta. Metall. 35 (1987) 2443.
[11] J.T.C. Lee, K. Tsiveriotis, R.A. Brown, J. Crystal Growth 121 (1992) 536.
[12] J.T.C. Lee, R.A. Brown, Phys. Rev. B 47 (1993) 4937.